Formation Control of Multiple Robots Based on Linearization Scheme

Wei Zhou, Hui Cheng*, Qiyuan Zhu, Zeyu Jiang

Department of Automation, Sun Yat-sen University, Guangzhou, China
E-mail: chengh9@mail.sysu.edu.cn

Abstract: In this paper, formation control of multi-robot systems based on the leader-follower scheme is studied by taking into account time-varying velocity of the leader as well as the unknown formation angle. In traditional leader-follower based formation control algorithms, control inputs are highly coupled. Moreover, the states of the robots ideally assumed to be known are usually hard to be measured or estimated using onboard sensors. With these issues considered, a novel algorithm based on linearization is proposed to adapt to the time-varying velocity of leader, and also to mitigate the coupling between control inputs. In addition, in order to increases the practicability of formation control algorithm and improves the performance of formation system, this paper design a state observer to estimate the formation angle, which cannot be measured. The numerical results illustrate that the proposed control algorithm can adapt to the time-varying velocity of the leader. Meanwhile, this algorithm can reduce the dependence on the system states being ideally known.

Key Words: Leader-Follower, Formation Control, Linearization, State Observer

1 INTRODUCTION

Cooperation of multiple robots can efficiently accomplish complicated missions compared with one single robot [1-2]. Formation control is essential to cooperative control of multi-robot systems [3-4]. Various formation control strategies have been presented for groups of robots. The leader-follower algorithms [5-7], the model predictive controller [8], the virtual-structure method [9], the behavior-base scheme [10] and the graph-based strategy [11] have been proposed in the literatures. The leader-follower algorithm aims to control the relative distances and angles among the leader and the followers. The leader-follower algorithm has been widely applied in formation control. V. J. Kumar et al. [5] [12] proposed two formation modes, l-ϕ and $l-l$, which utilize the traditional input-output linearization to design the control law, and the convergence of the proposed control law is analyzed. In [13], the concept of a virtual robot is presented based on the acquired global information. Moreover, a virtual leader controller is presented based on the cascade heteronomy system theory in order to make the formation converge more quickly. In [14], by introducing a new kinematics model for the leader-follower system using Cartesian coordinates, a globally stable controller is presented for formation control. Moreover, sliding mode control [15] and neural networks [16] are also adopted in the leader-follower strategies. In general, it is usually assumed that all information can be accessed in the multiple-robot systems. For example, the position and velocity of the robot in the world coordinate, the relative distances and angles among the robots are assumed to be perfectly known by measurement or communication. However, system states cannot be obtained sometimes, or the acquired states have estimation errors due to the noisy measurements or inherently unreliable wireless communication channels in practice. In these situations, the control algorithms based on the precise system states are not effective.

In conventional leader-follower based formation control algorithms, control inputs are highly coupled. Moreover, the assumption that the system states of the multi-robot system are ideally known cannot be met in practice. In this paper, a linearized formation controller is proposed. It mitigates the coupling between control inputs and is robust to the time-varying velocity of the leader. Moreover, when the relative angle between the leader and the follower cannot be measured, a state observer is presented to estimate the relative angle.

The rest of this paper is organized as follows. Section 2 formulates the problem. Section 3 proposes a linearized formation controller, and its convergence is proved. Section 4 presents a state observer to estimate the relative angle. In Section 5, simulation results are presented and analyzed. Section 6 concludes the paper.

2 PROBLEM FORMULATION

In this paper, we focus on four-wheel differential driving mobile robot. As shown in the Fig. 1, o is the center of mass of robot, and the distance between wheels is 2d. Let (x_i, y_i, θ_i) denote the position and orientation of the robot with respect to the world coordinate frame, and v_i and ω_i denote the linear and angular velocity of the robot. The kinematical model is given as follows:

$$\begin{bmatrix} \dot{x}_i \\ \dot{y}_i \\ \dot{\theta}_i \end{bmatrix} = \begin{bmatrix} \cos\theta_i & -d\sin\theta_i \\ \sin\theta_i & d\cos\theta_i \\ 0 & 1 \end{bmatrix} \begin{bmatrix} v_i \\ \omega_i \end{bmatrix} \tag{1}$$

The $l-\phi$ structure of the leader-follower formation scheme is shown in Fig.2. The leader moves along the desired route. Meanwhile, the follower tracks the leader to keep the desired relative distance/angle l/ϕ with respect

Research supported by the Science and Technology Program of Guangzhou under Grant 1563000439 and the Fundamental Research Funds for the Central Universities.

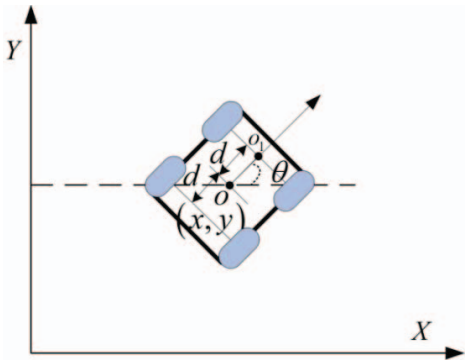

Fig. 1. The robot model.

to the leader. The desired relative distance and angle (l,ϕ) are determined based on the formation task. It is supposed that the leader and the follower can perceive each other's position and attitude using onboard sensors or by communication. $l-l$ is another leader-follower structure consisting of two $l-\phi$ structures. For a group of robots, the structures $l-\phi$ and $l-l$ can be considered for fromation control of subsystems. It is shown that the formation controller of a multi-robot system is stable if the subsystems are stable [11].

The desired distance and angle (l,ϕ) is:

$$\begin{cases} l=\sqrt{(x_1-x_2)^2+(y_1-y_2)^2} \\ \varepsilon_{12}=\arctan\left(\dfrac{y_1-y_2}{x_1-x_2}\right) \\ \phi=\pi-\theta_1+\varepsilon_{12} \end{cases} \tag{2}$$

and their derivatives are given as below:

$$\begin{cases} \dot{l}=-v_1\cos\phi-\omega_1 d\sin\phi+v_2\cos\gamma+\omega_2 d\sin\gamma \\ \dot{\phi}=(v_1\sin\phi-\omega_1 d\cos\phi-v_2\sin\gamma+\omega_2 d\cos\gamma \\ -l\omega_1)/l \\ \dot{\theta}_{12}=\dot{\theta}_1-\dot{\theta}_2=\omega_1-\omega_2 \\ \gamma=\theta_{12}+\phi \end{cases} \tag{3}$$

where $(x_1,y_1,\theta_1,v_1,\omega_1)$ denote the position and orientation of the leader, $(x_2,y_2,\theta_2,v_2,\omega_2)$ denote the position and orientation of the follower, and $\boldsymbol{u}=[u_1\ u_2]^{\mathrm{T}}=[v_2\ \omega_2]^{\mathrm{T}}$ denote the control inputs of the follower.

In addition, the linear and angular velocities of the leader are bounded, i.e.

$$0\le|v(t)|\le v_{\max},\ 0\le|\omega(t)|\le\omega_{\max} \tag{4}$$

where $v_{\max}$ and $\omega_{\max}$ are the maximum linear and angular velocities. The desired formation is $(l^{\mathrm{d}},\phi^{\mathrm{d}})$. So the aim of the leader-follower formation is to make relative distance and the relative angle (l,ϕ) between the leader and the follower converges to the desired formation.

$$\lim_{t\to\infty}(l-l^{\mathrm{d}})=0,\ \lim_{t\to\infty}(\phi-\phi^{\mathrm{d}})=0 \tag{5}$$

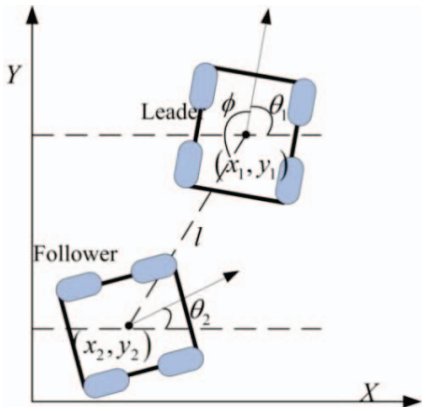

Fig. 2. The formation structure of two robots.

3 CONTROLLER DESIGN OF FORMATION

3.1 Input-Output Linearization Method

Input-output linearization is an effective method for controller design in nonlinear systems. The nonlinear system is linearized by output feedback, and the controller is designed base on the linear system theory. The control strategy can be expressed as:

$$\dot{l}=k_1\left(l-l^{\mathrm{d}}\right),\ \dot{\phi}=k_2\left(\phi-\phi^{\mathrm{d}}\right) \tag{6}$$

By combining Eqn. (3) with Eqn. (6), the control law can be obtained as follows:

$$\begin{cases} u_1=k_1e_1\cos\gamma-k_2le_2\sin\gamma-l\omega_1\sin\gamma \\ +v_1\cos\theta_{12}-d\omega_1\sin\theta_{12} \\ u_2=(k_1e_1\sin\gamma+k_2le_2\cos\gamma+l\omega_1\cos\gamma \\ -v_1\sin\theta_{12}+d\omega_1\cos\theta_{12})/d \end{cases} \tag{5}$$

where $k_1>0,k_2>0$ are positive gains, and $\boldsymbol{e}=[e_1\ e_2]^{\mathrm{T}}$ $=[l-l^{\mathrm{d}}\ \phi-\phi^{\mathrm{d}}]^{\mathrm{T}}$ denote formation errors.

It can be shown that the control inputs in Eqn. (7) are highly coupling as the formation distance and angle are dependent on one another. In addition, the states of the multi-robot system are generally assumed to be ideally known although the assumption cannot be met in practice.

3.2 Controller Design Base on Linearization

Considering the nonlinear system (3), we aim to design a controller $\boldsymbol{u}$ to stabilize it. Denote the state as $\boldsymbol{q}=[l\ \phi]^{\mathrm{T}}$ and its derivative $\dot{\boldsymbol{q}}=f(t,\boldsymbol{q},\boldsymbol{u})$. The equilibrium of the system is denoted as $\boldsymbol{q}^{\mathrm{d}}=[l^{\mathrm{d}}\ \phi^{\mathrm{d}}]^{\mathrm{T}}$. The control input $\boldsymbol{u}_{\mathrm{ss}}=[u_{1\mathrm{ss}}\ u_{2\mathrm{ss}}]^{\mathrm{T}}$ satisfies $\boldsymbol{0}=f\left(t,\boldsymbol{q},\boldsymbol{u}_{\mathrm{ss}}\right)\big|_{\boldsymbol{q}=\boldsymbol{q}^{\mathrm{d}}}$ and can be obtained as follows:

$$\boldsymbol{u}_{\mathrm{ss}}=\begin{bmatrix} v_1\cos\theta_{12}-dw_1\sin\theta_{12}-l^{\mathrm{d}}w_1\sin(\theta_{12}+\phi^{\mathrm{d}}) \\ \dfrac{1}{d}(v_1\sin\theta_{12}+dw_1\cos\theta_{12}+l^{\mathrm{d}}w_1\cos(\theta_{12}+\phi^{\mathrm{d}})) \end{bmatrix}$$

where $\boldsymbol{e}=\boldsymbol{q}-\boldsymbol{q}^{\mathrm{d}}=[e_1\ e_2]^{\mathrm{T}}=[l-l^{\mathrm{d}}\ \phi-\phi^{\mathrm{d}}]^{\mathrm{T}}$ are formation

errors. In order to control the equilibrium state to $(0,0)$, define the new control law as $\boldsymbol{u}_0 = \boldsymbol{u} - \boldsymbol{u}_{\rm ss} = [u_{01}\ u_{02}]^{\rm T}$, where $\boldsymbol{u}_0$ is linear feedback control corresponding to $\boldsymbol{e}$, and $\boldsymbol{u}_{\rm ss}$ is the feed-forward control input. By inserting $\boldsymbol{e}$ and $\boldsymbol{u}_0$ into Eqn. (3), the formation error vector $\boldsymbol{e}$ is given as:

$$\begin{cases} \dot{e}_1 = -v_1\cos\left(e_2+\phi^{\rm d}\right) - \omega_1 d\sin\left(e_2+\phi^{\rm d}\right) + \\ \left(u_{1ss}+u_{01}\right)\cos\left(\theta_{12}+e_2+\phi^{\rm d}\right) + \\ \left(u_{2ss}+u_{02}\right)d\sin\left(\theta_{12}+e_2+\phi^{\rm d}\right) - l^{\rm d} \\ \dot{e}_2 = \dfrac{1}{e_1+l^{\rm d}}\left(v_1\sin\left(e_2+\phi^{\rm d}\right) - \omega_1 d\cos\left(e_2+\phi^{\rm d}\right)\right. \\ -\left(u_{1ss}+u_{01}\right)\sin\left(\theta_{12}+e_2+\phi^{\rm d}\right) + \\ \left.\left(u_{2ss}+u_{02}\right)d\cos\left(\theta_{12}+e_2+\phi^{\rm d}\right)\right) - \omega_1 - \dot{\phi}^{\rm d} \end{cases} \tag{6}$$

i.e.

$$\dot{\boldsymbol{e}} = f\left(\boldsymbol{e}, \boldsymbol{u}_0\right) \tag{7}$$

According to nonlinear system stability theory [25], the nonlinear system (10) can be linearized as:

$$\dot{\boldsymbol{e}} = \boldsymbol{A}\boldsymbol{e} + \boldsymbol{B}\boldsymbol{u}_0 \tag{8}$$

where

$$\boldsymbol{A} = \frac{\partial f}{\partial \boldsymbol{e}}(\boldsymbol{e},\boldsymbol{u}_0)\big|_{\boldsymbol{e}=\boldsymbol{0},\boldsymbol{u}_0=\boldsymbol{0}} = \begin{bmatrix} 0 & l^{\rm d}\omega_1 \\ -\omega_1/l^{\rm d} & 0 \end{bmatrix}$$

$$\boldsymbol{B} = \frac{\partial f}{\partial \boldsymbol{u}_0}(\boldsymbol{e},\boldsymbol{u}_0)\big|_{\boldsymbol{e}=\boldsymbol{0},\boldsymbol{u}_0=\boldsymbol{0}} = \begin{bmatrix} \cos\left(\theta_{12}+\phi^{\rm d}\right) & d\sin\left(\theta_{12}+\phi^{\rm d}\right) \\ \dfrac{-\sin\left(\theta_{12}+\phi^{\rm d}\right)}{l^{\rm d}} & \dfrac{d\cos\left(\theta_{12}+\phi^{\rm d}\right)}{l^{\rm d}} \end{bmatrix}$$

Assume that $(\boldsymbol{A},\boldsymbol{B})$ is controllable [17], a linear feedback control law $\boldsymbol{u}_0 = -\boldsymbol{K}\boldsymbol{e}$ can be designed to stabilize the system (11) with

$$\boldsymbol{K} = -\begin{bmatrix} k_1 & k_2 \\ k_3 & k_4 \end{bmatrix},\quad \boldsymbol{e} = \begin{bmatrix} l-l^{\rm d} \\ \phi-\phi^{\rm d} \end{bmatrix}$$

The feedback control $\boldsymbol{u}$ is hence given as:

$$\boldsymbol{u} = \boldsymbol{u}_0 + \boldsymbol{u}_{\rm ss} \tag{12}$$

3.3 Stability Analysis

Theorem 1. With the formation controller (12), the formation errors will converge to zero asymptotically if the following conditions are met:

(1) The initial difference between the heading angles of the leader and the follower are bounded, i.e. $\theta_{12}|_{t=t_0} \in [-\pi/2, \pi/2]$.

(2) The elements of $\boldsymbol{K}$ satisfy $k_1 > 0$, $k_4 > 0$.

Proof: To verify the controllability of system (11), the rank of matrix $\boldsymbol{C} = [\boldsymbol{B}, \boldsymbol{A}\boldsymbol{B}]$ is considered, where

$$\begin{vmatrix} \cos\left(\theta_{12}+l^{\rm d}\right) & d\sin\left(\theta_{12}+l^{\rm d}\right) \\ \dfrac{-\sin\left(\theta_{12}+l^{\rm d}\right)}{l^{\rm d}} & \dfrac{d\cos\left(\theta_{12}+l^{\rm d}\right)}{l^{\rm d}} \end{vmatrix} = \frac{d}{l^{\rm d}} \neq 0 \tag{13}$$

In the matrix $\mathbf{C}$, the 2-order sub-determinant (13) is not equal to zero, and thus $\text{rank}(\boldsymbol{C}) \geq 2$. Meanwhile, the rank of the matrix $\mathbf{C}$ satisfies $\text{rank}(\boldsymbol{C}) \leq 2$. Therefore, it has $\text{rank}(\boldsymbol{C}) = 2$. The system (11) is controllable.

The linear feedback control law for the system (11) is $\boldsymbol{u}_0 = -\boldsymbol{K}\boldsymbol{e}$, and the closed-loop control system is

$$\dot{\boldsymbol{e}} = (\boldsymbol{A}-\boldsymbol{B}\boldsymbol{K})\boldsymbol{e} \tag{14}$$

If $\boldsymbol{A}-\boldsymbol{B}\boldsymbol{K}$ is a Hurwitz matrix [17], the closed-loop control system will converge asymptotically to zero. Specifically, its corresponding characteristic roots λ_1, λ_2 satisfy the following inequalities:

$$\begin{cases} \lambda_1 + \lambda_2 < 0 \\ \lambda_1\lambda_2 > 0 \end{cases} \tag{15}$$

Without loss of generality, assume $k_2 = k_3 = 0$ in the matrix $\boldsymbol{K}$. Then, the characteristic polynomial of $\boldsymbol{A}-\boldsymbol{B}\boldsymbol{K}$ can be expressed as:

$$\begin{aligned} \left|(\boldsymbol{A}-\boldsymbol{B}\boldsymbol{K}) - \lambda\boldsymbol{I}\right| &= \lambda^2 + \left(\frac{dk_4\cos\gamma_0}{l^{\rm d}} + k_1\cos\gamma_0\right)\lambda \\ &+ \left(\omega_1^2 + \frac{dk_1k_4}{l^{\rm d}} - \frac{dk_4\omega_1\sin\gamma_0}{l^{\rm d}} - k_1\omega_1\sin\gamma_0\right) \end{aligned} \tag{16}$$

where $\gamma_0 = \theta_{12} + \phi^{\rm d}$.

The characteristic polynomial can be analyzed as follows. If $dk_4/l^d = k_1$, it has

$$\begin{cases} \lambda_1 + \lambda_2 = -\left(\dfrac{dk_4\cos\gamma_0}{l^d} + k_1\cos\gamma_0\right) = -k_1\cos\gamma_0 \\ \lambda_1 * \lambda_2 = \omega_1^2 + \dfrac{dk_1k_4}{l^d} - \dfrac{dk_4\omega_1\sin\gamma_0}{l^d} - k_1\omega_1\sin\gamma_0 \\ \qquad = \omega_1^2 + {k_1}^2 - 2k_1\omega_1\sin\gamma_0 \geq \omega_1^2 + {k_1}^2 - 2k_1\omega_1 \\ \qquad = (\omega_1 - k_1)^2 \geq 0 \end{cases} \tag{17}$$

According to the above analysis, it can be known that if $k_1\cos\gamma_0 > 0$, the matrix $\boldsymbol{A}-\boldsymbol{B}\boldsymbol{K}$ is a Hurwitz matrix. Moreover, if the gains are set according to $k_1 = a\cos\gamma_0$, $a > 0$, and $k_4 = k_1 l^{\rm d}/d = a\cos\gamma_0 l^{\rm d}/d$, the closed-loop system (11) will converge asymptotically to zero,

When $k_2 \neq 0$ and $k_3 \neq 0$, the above analysis can be straightforwardly extended to show that the follower can maintain the desired formation relative to the leader and formation errors will converge asymptotically to zero.

The diagram of the formation controller based on linearization is shown in Fig. 3.

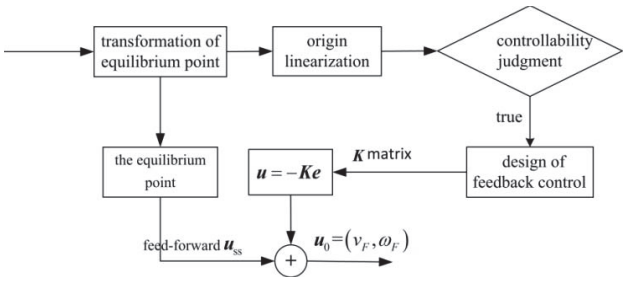

Fig. 3. Formation control based on Linearization.

4 STATE OBSERVER DESIGN BASED ON LINEARIZATION

The system states such as the relative distance l, the relative angle ϕ and the velocity of the leader need to be obtained in the leader-follower based formation controller. A multi-robot system can acquire partial system states with onboard sensing. However, the relative angle ϕ is difficult to measure using onboard sensors. When the relative angle ϕ is infeasible, a state observer is needed to be designed to ensure the effectiveness of the controller.

Let $\boldsymbol{q}=[l\ \phi]^{\mathrm{T}}$ denote the real system states, and $\hat{\boldsymbol{q}}=[\hat{l}\ \hat{\phi}]^{\mathrm{T}}$ denote the estimated system states. A state observer is designed to ensure the estimation converge to the real values asymptotically:

$$\lim_{t\to\infty}(\hat{\boldsymbol{q}}-\boldsymbol{q})=\boldsymbol{0} \tag{18}$$

where $\boldsymbol{e}=\boldsymbol{q}-\boldsymbol{q}^{\mathrm{d}}=[e_1\ e_2]^{\mathrm{T}}=[l-l^{\mathrm{d}}\ \phi-\phi^{\mathrm{d}}]^{\mathrm{T}}$ denote the errors between the current states and the desired states, $\hat{\boldsymbol{e}}=\hat{\boldsymbol{q}}-\boldsymbol{q}^{\mathrm{d}}=[\hat{e}_1\ \hat{e}_2]^{\mathrm{T}}=[\hat{l}-l^{\mathrm{d}}\ \hat{\phi}-\phi^{\mathrm{d}}]^{\mathrm{T}}$ are the estimation errors, and the observed state errors are $\tilde{\boldsymbol{e}}=\hat{\boldsymbol{e}}-\boldsymbol{e}=[\tilde{e}_1\ \tilde{e}_2]^{\mathrm{T}}=[\hat{l}-l\ \hat{\phi}-\phi]^{\mathrm{T}}$.

Define $\hat{\boldsymbol{u}}_{\boldsymbol{0}}=-\boldsymbol{K}\hat{\boldsymbol{e}}$. Eqn. (11) can be written as

$$\dot{\boldsymbol{e}}=\boldsymbol{A}\boldsymbol{e}+\boldsymbol{B}\hat{\boldsymbol{u}}_{\boldsymbol{0}} \tag{19}$$

Let $y=\boldsymbol{C}\boldsymbol{e}=[1\ 0]\boldsymbol{e}=e_1$ denote the measurable system state errors. The observer can be defined as:

$$\begin{aligned}\dot{\hat{\boldsymbol{e}}}&=\boldsymbol{A}\hat{\boldsymbol{e}}+\boldsymbol{B}\hat{\boldsymbol{u}}_0+\boldsymbol{H}(y-\hat{y})\\&=\boldsymbol{A}\hat{\boldsymbol{e}}+\boldsymbol{B}\hat{\boldsymbol{u}}_0+\boldsymbol{H}(y-\boldsymbol{C}\hat{\boldsymbol{e}})\\&=\boldsymbol{A}\hat{\boldsymbol{e}}+\boldsymbol{B}\hat{\boldsymbol{u}}_0+\boldsymbol{H}\boldsymbol{C}(\boldsymbol{e}-\hat{\boldsymbol{e}})\end{aligned} \tag{20}$$

where the matrix $\boldsymbol{H}=[h_1,h_2]^{\mathrm{T}}$ and $\hat{\boldsymbol{u}}_{\boldsymbol{0}}=-\boldsymbol{K}\hat{\boldsymbol{e}}$.

Theorem 2. With the system state observer (20), if $h_1>0$ and $h_2=\omega_1/l^{\mathrm{d}}$, the system observation errors will converge to zero asymptotically.

Proof: The estimation error $\hat{\boldsymbol{e}}=\hat{\boldsymbol{e}}-\boldsymbol{e}$ satisfies the following equation:

$$\dot{\tilde{\boldsymbol{e}}}=(\boldsymbol{A}-\boldsymbol{H}\boldsymbol{C})\tilde{\boldsymbol{e}} \tag{21}$$

It can be shown that the system (19) is observable. According to the Theorem 4.5 [17], when $\boldsymbol{A}-\boldsymbol{H}\boldsymbol{C}$ is a Hurwitz matrix, the estimation error converges asymptotically to zero, i.e. $\lim_{t\to\infty}\tilde{e}=0$, where

$$\boldsymbol{A}-\boldsymbol{H}\boldsymbol{C}=\begin{bmatrix}-h_1 & l^{\mathrm{d}}\omega_1\\ -\omega_1/l^{\mathrm{d}}-h_2 & 0\end{bmatrix} \tag{22}$$

Specifically, its characteristic roots satisfy the following inequalities:

$$\begin{cases}\lambda_1+\lambda_2<0\\ \lambda_1\lambda_2>0\end{cases} \tag{23}$$

The characteristic polynomial is obtained as follows:

$$\left|(\boldsymbol{A}-\boldsymbol{H}\boldsymbol{C})-\lambda\boldsymbol{I}\right|=\lambda^2+h_1\lambda+\omega_1\left(\omega_1+h_2l^{\mathrm{d}}\right) \tag{24}$$

It leads to

$$\begin{cases}\lambda_1+\lambda_2=-h_1\\ \lambda_1\lambda_2=\omega_1\left(\omega_1+h_2l^{d}\right)\end{cases} \tag{25}$$

If $h_1>0$ and $h_2=\omega_1/l^{\mathrm{d}}$, we have $\lambda_1+\lambda_2<0$ and $\lambda_1\lambda_2=2w_1^{\,2}\geq 0$. Hence, the system state estimation errors will converge to zero asymptotically.

The diagram of a closed-loop control system with the system state observer is shown in Fig. 4.

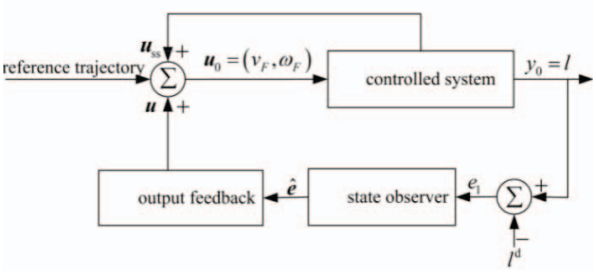

Fig. 4. Diagram of a closed-loop system with the state observer.

5 SIMULATION EXPERIMENTS

In this section, the performance of the formation control law (12) and the state observer (20) are studied via numerical simulations. The cases of asymptotic constant velocity and time-varying velocity of leader are considered, respectively. Moreover, the performance of the state observer is studied when the relative angle is infeasible.

Experiment 1: The desired trajectory of the leader is a circle, and the velocity of the leader is asymptotically constant. The linear velocity υ_{L} of the leader varies from $\sin(0.5t)$ to $1\mathrm{m/s}$, and the angular velocity is $\omega_{\mathrm{L}}=\upsilon_{\mathrm{L}}/3$. The control parameters are set as:

$$\upsilon_{\max}=2m/\mathrm{s},\ \omega_{\max}=0.5\,\mathrm{rad/s},\ d=0.1,\ a=10.$$

Table 1. Initial System States

$\mathbf{R}_1=[x_1(0)\ \ y_1(0)\ \ \theta_1(0)]^{\mathrm{T}}=[0\ \ 0\ \ \pi/2]^{\mathrm{T}}$
$\mathbf{R}_2=[x_2(0)\ \ y_2(0)\ \ \theta_2(0)]^{\mathrm{T}}=[-2.7\ \ -0.5\ \ \pi/3]^{\mathrm{T}}$

where $\mathbf{R}_i=[x_i(0)\ \ y_i(0)\ \ \theta_i(0)]^{\mathrm{T}}$, $i=1,2$ denote the initial states of the robots.

The formation parameters are shown in Table 2:

Table 2. Formation parameters

$[l_{12}^{\mathrm{d}}\ \phi_{12}^{\mathrm{d}}]^{\mathrm{T}}=[2\ \ \pi/3]^{\mathrm{T}}$, $[l_{12}(0)\ \phi_{12}(0)]^{\mathrm{T}}=[2.7\ \ 1.8]^{\mathrm{T}}$
$\boldsymbol{e}_{ij}(0)=\boldsymbol{q}_{ij}^{\mathrm{d}}-\boldsymbol{q}_{ij}(0)=[0.7\ \ 0.7]^{\mathrm{T}}$

where $\boldsymbol{q}_{ij}^{\mathrm{d}}$ denote the desired formation parameters, $\boldsymbol{q}_{ij}(0)$ denotes the initial formation, $\boldsymbol{e}_{ij}(0)$ denotes the initial formation error, and i and j stand for the leader an the follower, respectively.

The trajectories of the two robots are depicted in Fig. 5(b). When the velocity of leader is asymptotically constant, it is shown that from Fig. 5(b) that the follower can maintain the desired formation relative to the leader after a period of time. The relative distance and the angle errors are shown in Fig. 5(b) and Fig. 5(c). It is shown from Figs. 5(c) and (d) that the formation errors convergent to zero asymptotically.

Experiment 2: In this case, the desired path of the leader is a sine curve, the time-varying velocity of leader υ_{L} varies as a cosine function, and the angular velocity ω_{L} varies as a sine function. The control parameters are set as: $\upsilon_{\max}=1.5\,\mathrm{m/s}$, $\omega_{\max}=0.5\,\mathrm{rad/s}$, $d=0.1$, $a=12$.

Table 3. Initial System States

$\mathbf{R}_1=[x_1(0)\ \ y_1(0)\ \ \theta_1(0)]^{\mathrm{T}}=[0\ \ 0\ \ \pi/4]^{\mathrm{T}}$
$\mathbf{R}_2=[x_2(0)\ \ y_2(0)\ \ \theta_2(0)]^{\mathrm{T}}=[-0.6\ \ -0.85\ \ \pi/3]^{\mathrm{T}}$

Table 4. Formation Parameters

$[l_{12}^{\mathrm{d}}\ \phi_{12}^{\mathrm{d}}]^{\mathrm{T}}=[1\ \ \pi/4]^{\mathrm{T}}$, $[l_{12}(0)\ \phi_{12}(0)]^{\mathrm{T}}=[1.04\ \ 1.4]^{\mathrm{T}}$
$\boldsymbol{e}_{ij}(0)=\boldsymbol{q}_{ij}^{\mathrm{d}}-\boldsymbol{q}_{ij}(0)=[0.04\ \ 0.61]^{\mathrm{T}}$

The trajectories of the two robots are depicted in Fig. 6(b). When the velocity of the leader is time-varying, it is shown that the follower maintain the desired formation relative to the leader. As shown in Figs. 6(c) and (d), the formation errors approximate to zero.

Experiment 3: In this case, the relative angle between the leader and the follower is assumed to be unknown and is estimated by the state observer. Similarly, the linear velocity υ_{L} varies as a cosine function, and the angular velocity ω_{L} varies as a sine function. The Control parameters are set as $\upsilon_{\max}=1.5\,\mathrm{m/s}$, $\omega_{\max}=0.5\,\mathrm{rad/s}$, $d=0.1$, $a=15$ and $h_1=10$. The initial system states and the formation parameters in this case are the same as those in the Experiment 2. The measured relative distance is noisy with Gaussian white noise with zero mean and variance of 0.2.

The trajectories of the two robots are depicted in Fig. 7(a). As demonstrated in Figs. 7(b) and (c), the system state observer can estimate the relative distance and angle accurately. Although the relative angle is infeasible and the measured relative distance is noisy, it is shown from Fig. 7 that the follower can maintain the desired formation relative to the leader after a period of time.

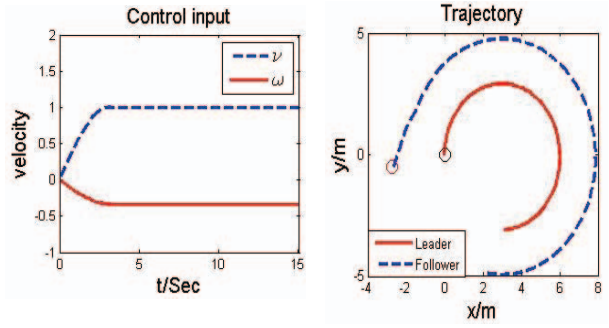

(a) Control input of leader

(b) Trajectories of robots

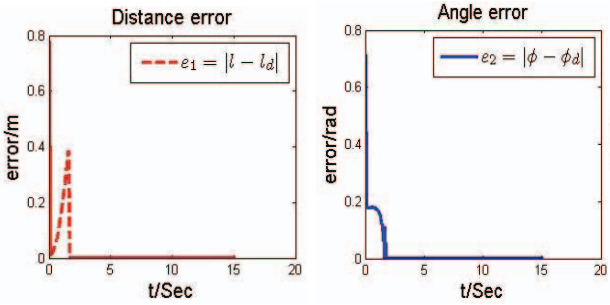

(c) Relative distance error

(d) Relative angle error

Fig. 5. Performance of the formation controller in the case of asymptotic constant velocity of the leader.

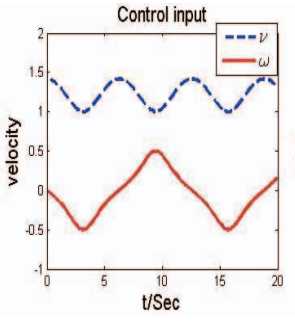

(a) Control input of leader

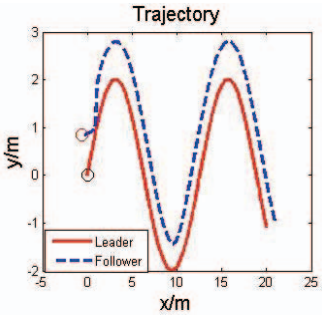

(b) Trajectories of robots

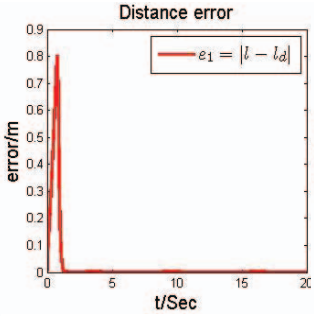

(c) Relative distance error

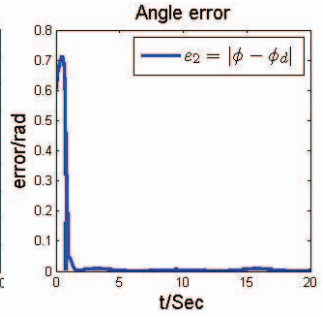

(d) Relative angle error

Fig. 6. Performance of the formation controller in the case of time-varying velocity of leader.

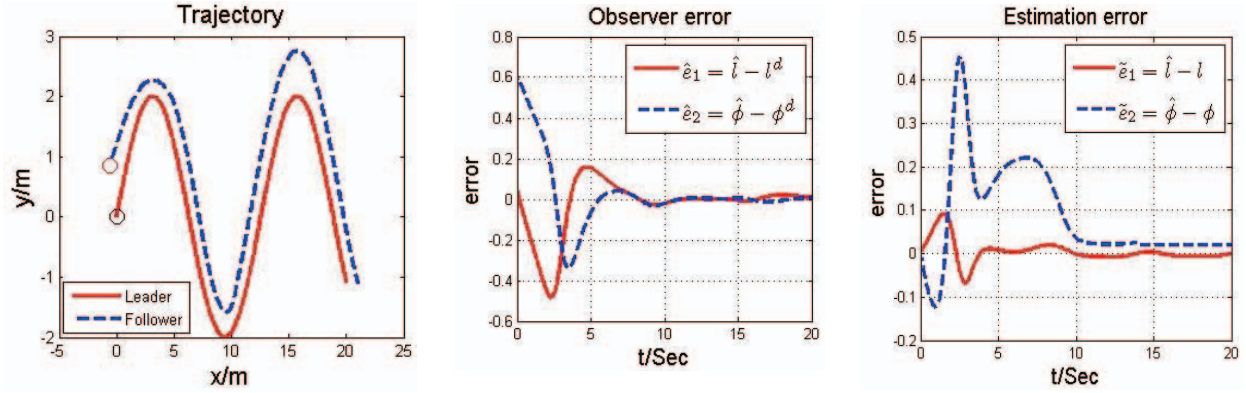

(a) Trajectory of two robots (b) Formation errors (c) Estimation errors

Fig. 7. Performance of the formation controller with the state observer.

6 CONCLUSION

In this paper, a novel formation control algorithm based on linearization has been proposed to adapt to the time-varying velocity of the leader, and to mitigate the coupling between control inputs. When the relative angle between the leader and the follower is infeasible and the measured relative distance is noisy, a state observer is presented. Simulation results illustrate that the proposed control strategy can keep the desired formation in the case of time-varying velocity of the leader; in addition, the follower can track the leader with the state observer in the case of unknown relative angle. In the future work, robust estimation of the velocity of the leader will be studied. Vision based formation control will be examined. Moreover, adaptive formation control will be studied to achieve specified tasks.

REFERENCES

[1] J. Pan, Nonlinear formation control of unicycle-type mobile robots. Robotics and Autonomous Systems, Vol.55, No.3, 191-204, 2007.

[2] L. Consolini, F. Morbidi, D. Prattichizzo and M. Tosques, stabilization of a hierarchical formation of unicycle robots with velocity and curvature constraints, IEEE Transactions on Robotics, Vol.25, No.5, 1176-1184, 2009.

[3] J. Wang, M. Obeng, T. Yang, G. Staskevich and B. Abbe, formation control of multiple non-holonomic mobile robots with limited information of a desired trajectory, Proceedings of IEEE International Conference on Electro Information Technology, 550-555, 2014.

[4] J. Rodrigues, D. Figueira, C. Neves and I. Ribeiro, leader-following graph-based distributed formation control, Proceedings of Robotica 8th Conference on Autonomous Robot Systems and Competitions, 71-77, 2008.

[5] J. Desai, a graph theoretic approach for modeling mobile robot team formations, Journal of Robotic Systems, Vol.19, No.11, 511-525, 2002.

[6] D. Aveek, F. Rafael, K. Vijay, O. James, S. John, T. Camillo, a vision-based formation control framework. IEEE Transactions on Robotics and Automation, Vol.18, No.5, 813-825, 2002.

[7] T. Herbert, P. George and K. Vijay, leader-to-formation stability, IEEE Transactions on Robotics and Automation, Vol.20, No.3, 443-455, 2004.

[8] S. Ferik, B. Siddiqui and F. Lewis, distributed non-linear MPC formation control with limited bandwidth, Proceedings of IEEE American Control Conference, 6388-6393, 2013.

[9] R. Beard and W. Ren, formation feedback control for multiple spacecraft via virtual structures, IET Control Theory and Applications, Vol.5, No.3, 357-368, 2004.

[10] J. Lawton, A. Beard and S. Member, a decentralized approach to formation maneuvers, IEEE Transactions on Robotics and Automation, Vol.19, No.6, 933-941, 2003.

[11] R. Olfati-Saber and R. Murray, graph rigidity and distributed formation stabilization of multi-vehicle systems, Proceedings of IEEE International Conference on Decision and Control, 2965-2971, 2002.

[12] J. Desai, J. Ostrowski and V. Kumar, modeling and control of formations of non-holonomic mobile robots. IEEE Transactions on Robotics and Automation, Vol.17, No.6, 905-908, 2001.

[13] T. Petrinic and I. Petrovic, a leader-follower approach to formation control of multiple non-holonomic mobile robots, Proceedings of IEEE Information & Communication Technology Electronics & Micro-electronics, 931-935, 2013.

[14] X.-H. Li, J.-Z. Xiao and Z.-J. Cai, backstepping based multiple mobile robots formation control, Proceedings of IEEE International Conference on Intelligent Robots and Systems, 887-892, 2005.

[15] D. Shen, Z. Sun and Y. Qiao, second-order sliding mode control for non-holonomic mobile robots formation. In: Proceedings of the 30th Chinese Control Conference, 4860-4864, 2011.

[16] J. Ni and S.X. Yang, bioinspired neural network for real-time cooperative hunting by multi-robots in unknown environments, IEEE Transactions on Neural Networks, Vol.5, No.3, 2062-2077, 2011.

[17] H. K. Khalil, Nonlinear Systems, Prentice-Hall, Third Edition, New Jersey, USA, 2001.